scientific reports

Check for updates

OPEN

Triaxial compression and shear strength characteristics of two-stage concrete: an experimental study

Farzam Omidi Moaf[1], Ali M. Rajabi[2], Hakim S. Abdelgader[1,3]✉, Marzena Kurpińska[1], G Murali[4,5] & Mikołaj Miśkiewicz[1]

The research necessity stems from the need to understand and evaluate the performance of Two-Stage Concrete (TSC) under triaxial compression conditions, as prior studies have predominantly focused on uniaxial and biaxial testing of conventional concrete (CC). This study represents the first comprehensive investigation into the triaxial compressive strength and related mechanical properties of TSC, addressing a critical gap in the existing body of literature. Three different mixtures were prepared, including one CC and two TSC variants with varying cement content. The results and behavior of these mixtures were compared to assess their performance. Findings reveal that TSC, particularly those types with finer aggregates, demonstrates superior shear strength, achieving up to 52.4 MPa under dry conditions, in contrast to the 48.38 MPa observed in CC. Furthermore, TSC exhibits remarkable stress tolerance, withstanding up to 82.04 MPa, significantly outperforming CC, which withstands only 69.61 MPa under similar conditions. This behavior can be attributed to the higher coarse aggregate content, the increased interaction and contact points between coarse aggregates, the improved bonding between them, and the inherent properties of the grout. TSC also maintains a higher modulus of elasticity and internal friction angles, indicating superior deformation behavior and shear resistance. Additionally, TSC shows greater resilience to moisture, suggesting its potential suitability for use in variable moisture environments. These properties highlight the strength of TSC for high-load applications and its suitability for infrastructure prone to environmental fluctuations.

Keywords Two-stage concrete, Shear Strength, Triaxial Compressive Strength, Cohesion, Internal friction, Stress

Two-Stage Concrete (TSC), also known as Colcrete, prepacked concrete, and preplaced aggregate concrete (PAC), is a unique type produced using a specialized technique that distinguishes it from conventional concrete[1]. TSC is an innovative type of concrete that necessitates a reduced amount of cement[2]. PAC is fabricated by placing coarse aggregates of varying sizes and shapes into formworks. The voids and gaps within the aggregates are then filled with a highly fluid grout mixture composed of cement and sand[3]. Due to the pre-placement of coarse aggregates, they account for approximately 60–70% of the total volume, leaving 30–40% of the volume as voids[4]. It is essential to fill these voids with grout[5]. A higher proportion of coarse aggregate reduces the amount of cement required compared to traditional concrete. These factors contribute to TSC's cost-effectiveness and capacity to minimize heat generation during hydration and reduce the likelihood of drying shrinkage[6]. Additionally, TSC exhibits desirable properties such as minimal volume change and strong adhesion, making it well-suited for repair projects[7]. Technological advancements in two-stage concrete are directed towards optimizing its performance characteristics and broadening its range of applications[4]: (i) TSC construction improves structural integrity and durability by pouring a high-strength base layer, partially cured before adding a second, specialized layer. This method enhances the concrete's resistance to abrasion and environmental conditions while providing robust structural support. (ii) Using a two-stage procedure can effectively manage temperature gradients and

[1]Faculty of Civil and Environmental Engineering, Gdansk University of Technology, Gdansk, Poland. [2]Engineering Geology Department, School of Geology, University of Tehran, Tehran, Iran. [3]Faculty of Engineering, Civil Engineering Department, University of Tripoli, Tripoli, Libya. [4]Institute of Energy Infrastructure, Universiti Tenaga Nasional, Jalan IKRAM-UNITEN, Kajang 43000, Selangor, Malaysia. [5]Centre of Research Impact and Outcome, Chitkara University, Rajpura 140417, Punjab, India. ✉email: h.abdelgader@uot.edu.ly

reduce the risk of thermal cracking. The first stage controls heat generation during hardening, while the second layer provides additional insulation and protection. (iii) The two-stage technique allows for precise control over concrete properties. The lower layer can be designed for structural strength and load-bearing capacity, while the upper layer can be tailored for aesthetic enhancements, including color and texture. TSC technology generally offers considerable advantages, particularly when enhanced performance, durability, and aesthetic quality are critical.

Initially, TSC was used to repair bridges and tunnels. Later applications of TSC concrete, known as massive element construction, include the construction of the Hoover Dam on the Colorado River at the border between Nevada and Arizona in the United States, between 1931 and 1936 [8]. In 1937, Lee Turzillo and Luis S. Wertz first applied TSC for tunnel repair in California and in 1946 for dam repair in the upper Colorado River, where the repair had to be performed underwater[7]. It is possible to use reinforcement, and the void spaces are filled with grout as shown in Fig. 1. The grout can also be injected under pressure[9]. The method of laying the mortar depends on the dimensions and shape of the element and the size of the coarse aggregate grains. Research on TSC concerning the use of various types of coarse aggregate has been conducted by several authors[10,11]. Ichino et al.[12] performed a series of uniaxial compressive and splitting tensile tests on TSC, employing eleven distinct glass coarse aggregates. These aggregates differed in shape, size, and surface texture. An increase in grout strength, coupled with enhanced surface roughness of the coarse aggregate, has been observed to significantly improve the bonding between the two materials, thereby augmenting the uniaxial compressive strength. Compared to crushed glass plate aggregate, spherical glass aggregate typically results in a higher modulus of elasticity in TSC and conventional concrete. Das et al.[13] demonstrated that reducing the coarse aggregate size from 20 mm to 10 mm led to a 20% increase in TSC compressive strength, while incorporating 10% silica fume resulted in a 12% enhancement. Incorporating silica fume into the TSC increased pull-off strength, irrespective of the coarse aggregate size, analogous to the improvements in compressive strength and splitting tensile strength. Specifically, adding silica fume yielded an approximate 57% enhancement in binding strength. Das et al.[14] conducted a study on the properties of TSC, incorporating silica fume (SF) and ground granulated blast furnace slag as partial replacements for cement, with substitution levels ranging from 0 to 10% for silica fume and 0–40% for slag. The results indicate that the compressive and splitting tensile strengths of TSC with 40% slag and 10% silica fume are comparable to, or even exceed, those of TSC without any additional cementitious materials. Esmaeili and Amiri[15] determined that adjusting the water-to-cement ratio in the mortar within the range of 0.3 to 0.5 achieved an optimal fluidity time of at least 70 s for the injectable mortar samples. At a water-to-cement ratio of 0.4 and a cement content of 800 kg/m^3, the mortar attained a maximum compressive strength of 28.88 MPa after 28 days, while the flexural strength reached 6.57 MPa.

Li et al.[16] discovered that two-stage ultra-high performance concrete represents an innovative material concept, characterized by the use of a minimal binder quantity (as low as 364 kg/m^3), a substantial volume of coarse aggregate, and a highly efficient binder. This is achieved through the two-stage method and high-performance grout, resulting in a compressive strength of up to 151.8 MPa after 91 days. Bayer[17] investigated the variations in TSC compressive strength resulting from the incorporation of mineral admixtures such as rock powder, slag, and fly ash. After 28 days, the combination with 50% slag as a partial cement substitute exhibited the highest compressive strength. Several investigations have examined the mechanical properties of TSC with various fibers and different types of concrete using this concept, and all have reported positive results in TSC[18–20]. Ichino et al.[21] found that the crater's dimensions, including both diameter and depth, remain relatively consistent for cases where the compressive strength exceeds 17.6 MPa, despite increases in compressive strength. The smallest spall diameter and depth are observed at a compressive strength of 30.6 MPa. As the compressive strength increases, spall depth and diameter increase slightly. According to the experimental results, it is advisable to exercise the same caution when using high-strength TSC for protective constructions as with high-strength conventional concrete.

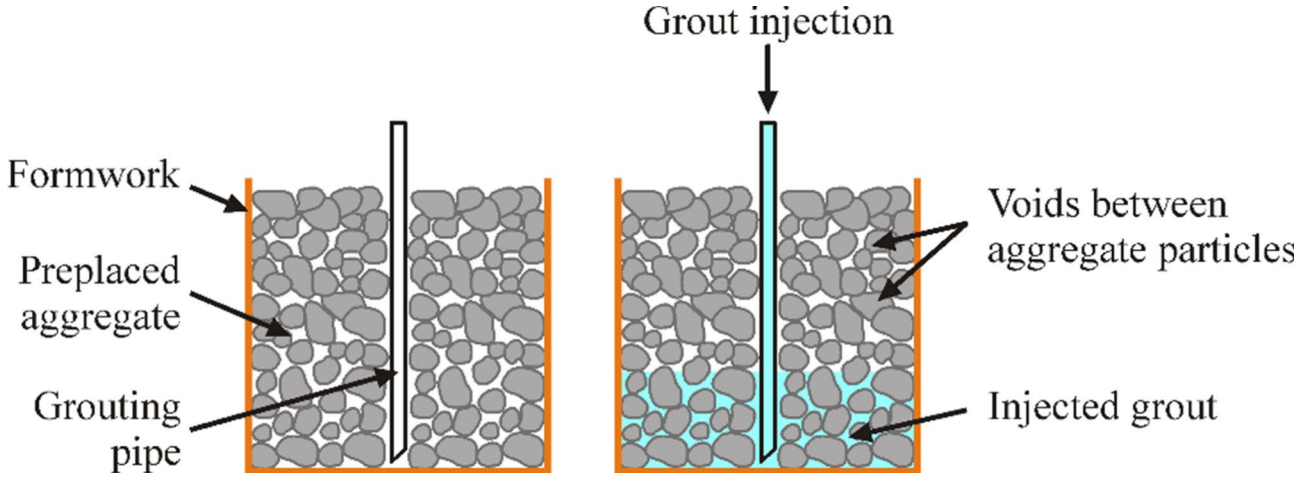

Fig. 1. TSC production process [Figure sourced from Najjar et al.[4]]

The study of concrete under triaxial compression represents an advanced research method that provides a more precise understanding of concrete's behavior when subjected to loads simultaneously applied in three directions. Unlike the standard uniaxial compression test, which assesses the material's resistance to compression along a single axis, triaxial compression testing provides insights into concrete's mechanical properties when simultaneously compressed in three perpendicular directions[22]. Triaxial compression studies enable a deeper understanding of concrete mechanics, including better characterization of its strength, deformability, and cracking. This analysis is particularly relevant in the context of real-world operational conditions, where building materials often undergo complex loads[23,24]. Accurate data on concrete behavior under triaxial loads are crucial for more precise structural element modeling and project optimization regarding safety and cost analysis[25]. Liu et al.[26] demonstrated that increasing confining pressure restricted the radial dilation of samples. Under triaxial shear loading, foamed concrete exhibited a reduction in volumetric strain. For every 0.1 MPa increase in confining pressure, there was an average increase of 0.075 MPa in peak strength and 0.16 MPa in residual strength. As the density of the foamed concrete increased, its compressive strength also rose; however, a decrease in silt content resulted in reduced strength. Ashrafi and Farzam[27] observed that the maximum stress and strain along the axis, significantly influenced by the degree of lateral confinement, were higher in triaxial compression tests compared to uniaxial and biaxial compression tests for lightweight aggregate concrete.

The novelty of this research lies in its comprehensive investigation of TSC under a triaxial compression scheme, particularly focusing on triaxial compressive strength tests conducted under various loading conditions. Numerous studies have investigated the mechanical properties of TSC with and without fibers; however, research on this specific topic, particularly under triaxial compression conditions, has not been previously conducted. This study is unique in presenting for the first time and comparative analyses of cohesion and internal friction angle alongside these tests. Additionally, it includes comparative testing on samples of ordinary concrete with the same compressive strength, providing a thorough evaluation of TSC's performance in different contexts.

Materials and methods

This investigation assessed the shear strength parameters of TSC, particularly types PA1 and PA2, compared to CC through triaxial compressive strength tests. In accordance with ASTM standards[28,29], a total of eighteen cylindrical specimens with dimensions of 150 mm in diameter and 300 mm in height were fabricated for uniaxial compressive strength testing. For triaxial tests, smaller cores measuring 50 mm in diameter and 100 mm in height were extracted from these primary specimens, adhering to the relevant ASTM guidelines[28,30] and the operational requirements of the triaxial testing apparatus employed in this study. Distinctive features of TSC samples included variable gravel granulation, contrasting with the standardized gravel used in CC. The TSC specimens utilized a specialized grout mixture, composed of Shahrood type 2 cement augmented with E.M. GROUT_500 expanding additive, to ensure cohesive aggregate integration. The application of triaxial stress, facilitated by a hydraulic cell, allowed for precise measurement of critical parameters such as cohesion and internal friction angle, which were meticulously analyzed with RocData software. This study aimed to scrutinize TSC's performance under various lateral stresses, directly comparing it to the benchmark set by CC. Despite uniform sand characteristics across all samples, the sand granulation varied between TSC and CC due to their differing fabrication methods. This variance is depicted in the aggregate grading curve illustrated in Fig. 2. Potable water and Shahrood type 2 cement were used to prepare the samples for all mixtures. The grout for

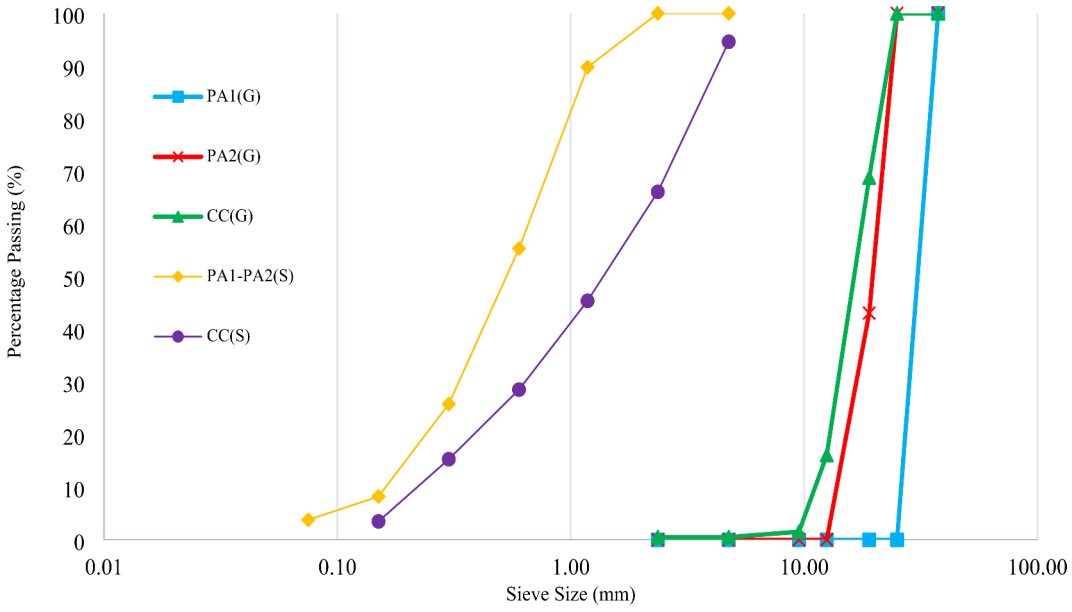

Fig. 2. The gradation curve for the aggregates.

TSC specimens additionally included the E.M. GROUT_500 additive to enhance performance characteristics, as detailed in Table 1.

The mixing ratio for TSC grouts is the same for PA1 and PA2, except for coarse aggregates. Normal concrete samples were mixed based on standard proportions for a cement content of 300 kg/m2. The TSC specimens were made by placing a predefined volume of aggregates in the molds, then filled with grout through a vibrating table, ensuring uniform distribution and compaction, as shown in Fig. 3. The void ratio in PA1 and PA2 is 0.41 and 0.38, respectively, and this space between the aggregates was filled with mortar. The details of ingredients for TSC and CC per cubic meter is shown in Table 2 and highlight the careful approach to mix design. After preparation, all samples were subjected to a 28-day curing period in water and followed standard conditioning protocols. TSC contains microscopic pores and capillaries within its matrix, particularly in the cement paste and around aggregates. These tiny voids can absorb water, allowing the concrete to become saturated when submerged in water for 28 days or exposed to high humidity.

Triaxial compressive strength tests simulated the complex stress conditions typically encountered by concrete in situ. The experimental design encompassed a wide array of samples, including both dry and saturated states for PA1, PA2, and CC, ensuring a comprehensive evaluation across varied environmental conditions. The samples prepared for triaxial testing and the testing apparatus itself are showcased in Figs. 4 and 5, respectively. The device in Fig. 5 is a three-axis testing machine designed for stone and concrete samples. These machines determine the mechanical properties of rock and concrete under triaxial stress conditions and provide vital information for construction and engineering projects.

The mohr-Coulomb failure criterion was introduced to rock mechanics by Jaeger[31] in 1959 by combining the work of Mohr and Coulomb. This criterion states that the cohesion of the material restricts shear failure across a plane. This criterion can be expressed mathematically as follows:

$$\tau = c + \sigma \ tan\varnothing \tag{1}$$

where, τ and σ are the shears and normal stresses, respectively, c is the apparent or inherent cohesion and $\varnothing$ is the angle of internal friction. The evaluation of the Mohr-Coulomb failure criteria requires many triaxial tests on rock samples at various confining pressures[32].

From Mohr's circle we have:

$$\sigma = \sigma_m - \tau_m \sin\varnothing ; \tau = \tau_m \cos\varnothing \tag{2}$$

Where.

$$\sigma_m = \frac{\sigma_1 + \sigma_3}{2}; \tau_m = \frac{\sigma_1 - \sigma_3}{2} \tag{3}$$

And σ_1 is the maximum principal stress and σ_3 is the minimum principal stress. Therefore, the Mohr-Coulomb criterion may also be expressed in the equation as follows[33].

$$\tau_m = \sigma_m \sin\varnothing + ccos\varnothing \tag{4}$$

SPECIFICATION of Cement											
PHYSICAL SPECIFICATION						CHEMICAL SPECIFICATION					
No.	Test	Result	Factory standard	INSO 389	Test Method	NO.	Component	Result (%)	Factory standard	INSO 389	Test Method
1	Fineness by Blaine (cm^2/gr)	2700	Min2600	Min2600	390	1	SiO_2	21.11	Max 20.5	-	1692
2	Autoclave expansion	0.046	Max 0.6	Max 0.8	391	2	Al_2O_3	4.48	Max 5	Max 6	
3	Setting time					3	Fe_2O_3	3.91	Max 5	Max 6	
3 – 1	Initial Time (min)	135	Min 70	Min 45	392	4	CaO	63.36	-	-	
3 – 2	Final time (min)	215	Max 300	Max 375	392	5	MgO	1.37	Max 2.5	Max 6	
4	Compressive Strength (MPa)					6	SO_3	2.58	Max 2.9	Max 3	
4 – 1	1 Day	-	-	-	393	7	Na_2O	0.43	-	-	1695
4 – 2	2 Day	19.12	-	-	393	8	K_2O	0.48	-	-	
4 – 3	3 Days	22.06	Min 16.67	-	393	9	L.O.I	2.85	Max 2.9	Max 3	1692
4–4	7 Days	31.87	Min 24.52	Min 17.65	393	10	IR	0.55	Max 0.1	Max1.5	
4–5	28 Days	36.77	Min 34.32	Min 31.87 Min 51.48	393	11	F. CaO	1.23	-	-	
5	Heat of hydration (cal/gr)					12	C3S	52.8	-	-	
5 – 1	3 Days	-	-	-	394	13	C2S	21	-	-	
5 – 2	28 Days	-	-	-	394	14	C3A	5.3	-	-	

Table 1. The specification of cement (shahrood type 2).

Fig. 3. Injection of grout into the gravels to build a TSC sample.

Employing the Mohr-Coulomb failure criterion, the study assessed shear failure across different planes, calculating the cohesion and angle of internal friction for each concrete type under stresses of 5.5, 7.5, and 10 MPa.

Results and discussions

Triaxial compressive strength testing yielded significant insights into the performance of PA1 and PA2 compared with CC across various conditions. The compiled data, detailed in Table 3, highlights the differential

Type of concrete	Name of Sample	W/C*	G (kg)	C (kg)	S (kg)	W (kg)	EA/C
TSC	PA1	0.5	1510	336	336	168	0.008
	PA2	0.5	1610	304	304	152	0.008
CC	CC	0.57	1225	300	630	170	0

Table 2. Details of ingredients and mix design. Note: W: water, C: cement, G: gravel, S: sand, EA: expanding admixture, CC: conventional concrete.

Fig. 4. Samples prepared for a triaxial experiment whose mosaic form is completely clear.

performance between the concrete types under dry and saturated conditions, specifically emphasizing strength values, cohesion (C), and internal friction angles (ϕ). Following the completion of the tests, the results were analyzed using Rock Data software, and the stress values for each sample were calculated. The Mohr-Coulomb method was employed, and the principal stresses (σ1 and σ3) were derived from the Mohr's circles.

Strength performance analysis

Under dry conditions, PA2 consistently exhibited the highest strength values across all test moduli (5, 7.5, and 10 MPa), suggesting its superior structural integrity compared to PA1 and CC. Interestingly, this trend persisted under saturated conditions, with PA2 displaying remarkable resilience. Notably, the transition from dry to saturated states resulted in a general decrease in strength for all concrete types, yet PA2's performance remained robust, underscoring its potential for applications in environments subject to moisture variation.

Cohesion and internal friction angle

Cohesion values for PA1 and CC remained relatively stable across different conditions and stress levels, indicating a consistent internal binding strength. In contrast, PA2 showed a slight increase in cohesion values when dry, suggesting an enhanced interparticle bond strength in the absence of moisture. The internal friction angle, a critical parameter for understanding material resistance to shear under load, was highest in PA2, especially in dry conditions. This indicates a superior shear resistance and a potential for PA2 to perform well in applications requiring high shear strength. The lower ϕ values in saturated conditions across all samples highlight the impact of moisture on shear resistance, a critical consideration for construction in variable moisture environments.

Figure 6 presents the internal friction angles for PA1, PA2, and CC under both dry and saturated conditions, illustrating the marked differences in their mechanical behavior when subjected to varying moisture levels. In the dry state, PA2 exhibits the highest friction angle, approximately 51 degrees, compared to PA1 at 44.9 degrees and CC at 46.4 degrees. This superior friction angle in PA2 suggests that its microstructural composition—potentially characterized by stronger inter-particle bonds and a more cohesive aggregate-cement interface, facilitates enhanced shear resistance. Such properties are particularly important in applications subject to high shear forces, as they contribute to the material's ability to resist deformation and failure under stress. Conversely, when saturated, all three materials show a reduction in their internal friction angles. PA2 decreases to approximately 42.7 degrees, PA1 to 40.1 degrees, and CC to 43.8 degrees. The most significant reduction is observed in PA2 (approximately 16%), highlighting the detrimental impact of moisture on the material's

Fig. 5. A three-axis testing machine designed for stone and concrete samples made by Heicoin company. **a.** Triaxial cell (Sample chamber), **b.** Hydraulic load frame, **c.** Dial gauge/displacement sensor, **d.** Pressure gauges and valves, **e**. Loading piston.

mechanical performance. The decline in friction angles under saturated conditions is primarily attributed to the weakening of the mechanical interlock between the aggregate particles and the cement matrix. The presence of water within the microstructure acts as a lubricant, facilitating relative motion between the particles and reducing the frictional resistance, which is critical for shear strength. Furthermore, the reduction in friction angles under saturated conditions emphasizes the critical need for designers and engineers to account for environmental

Sample name	Test Mode	σ_3(MPa)	$\sigma_1 - \sigma_3$ (MPa)	σ_1(MPa)	Mohar-Columb	
					C(MPa)	ϕ(deg)
PA1	Dry	5	43	48	3.6	44.9
		7.5	50	57.5		
		10	67	77		
PA2		5	47.4	52.4	2.4	51
		7.5	67.32	74.85		
		10	82.04	92.04		
CC		5	43.38	48.38	3.3	46.4
		7.5	54.12	61.62		
		10	69.61	79.61		
PA1	Saturate	5	34	39	3.5	40.1
		7.5	40.9	48.4		
		10	52.1	62.1		
PA2		5	42.07	47.07	4.7	42.7
		7.5	54.7	62.2		
		10	63.11	73.11		
CC		5	40.28	45.28	3.6	43.8
		7.5	48.33	55.83		
		10	62.79	72.79		

Table 3. Results of the three-axis compressive strength test.

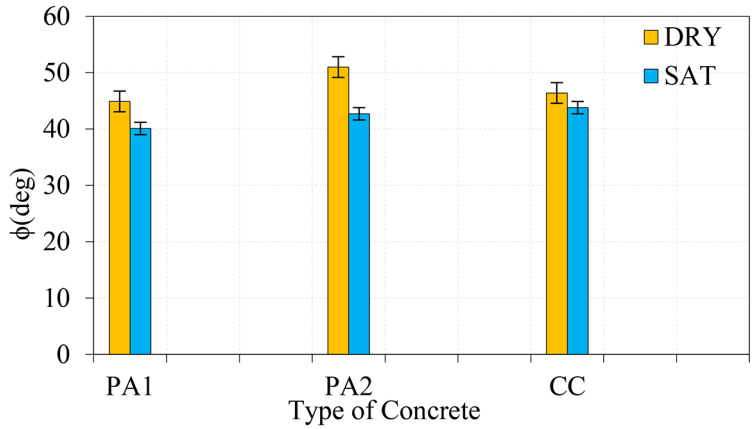

Fig. 6. Internal friction angle (φ) of concrete samples in a dry and saturated state.

factors such as moisture content and water ingress when selecting materials for construction. This is particularly relevant in areas with high humidity or frequent wet conditions, where moisture can significantly alter the mechanical properties of materials. The insights gained from this analysis are therefore crucial for understanding how material composition and environmental exposure can influence the long-term durability and performance of concrete, guiding the selection of appropriate materials for specific engineering applications.

Figure 7 presents an analysis of the cohesion values for three TSC materials: PA1, PA2, and CC, evaluated under both dry and saturated conditions. The data reveals notable disparities in cohesion, with PA2 demonstrating the cohesion in the dry state at 2.4 MPa, PA1 at 3.6 MPa and CC at 3.3 MPa. The superior cohesion of PA1 in the dry state suggests enhanced internal binding, reflecting its superior resistance to cracking and better capacity to bear load. This elevated cohesion in PA1 is likely attributed to an optimized interaction between the aggregate and cementitious matrix, potentially resulting from stronger chemical bonds or a finer particle distribution, which collectively contribute to its greater structural integrity under stress. On the other hand, PA1's cohesion in the dry state is lower than PA2's, yet still notable at 3.6 MPa. This suggests that PA1, while not as cohesive as PA2, still exhibits good inter-particle bonding, offering reasonable resistance to stress and cracking in dry conditions. The performance of CC, with a cohesion value of 3.3 MPa, is the lowest among the three materials, reflecting its relatively weaker internal bonding strength. The lower cohesion in CC is indicative of less effective particle interaction within the cement matrix, making it more prone to degradation under load compared to PA1 and PA2.

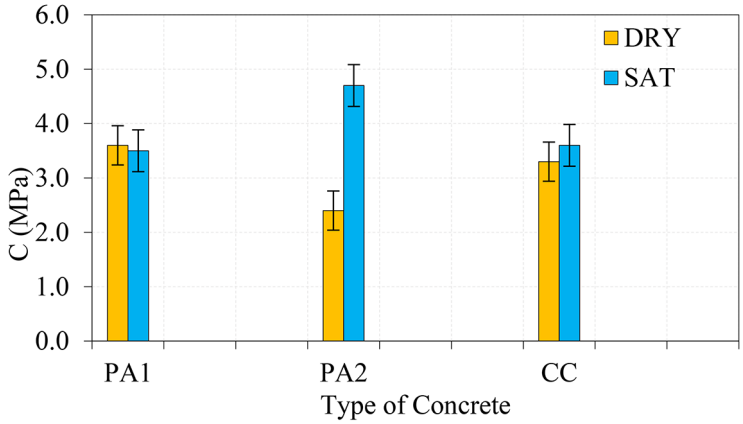

Fig. 7. Cohesion (C) of concrete samples in a dry and saturated state.

Upon saturation, with PA2 demonstrating a marginal increase to 4.7 MPa, while PA1's cohesion declines to 3.5 MPa, and CC experiences a slight increase to 3.6 MPa. The modest rise in cohesion observed for PA2 suggests that its internal structure may possess a greater resilience to moisture-induced alterations compared to the other two materials. This increase, though minor, may result from the redistribution of water within the microstructure, which could enhance the bond between cement and aggregate, thereby reducing the typical lubricating effect of water between particles. In contrast, PA1 experiences a noticeable reduction in cohesion upon saturation, with a drop to 3.5 MPa. This decrease suggests that PA1 is more sensitive to moisture exposure than PA2, with water potentially acting as a lubricant that weakens the inter-particle friction and reduces the material's cohesive strength. The reduction in cohesion in PA1, though moderate, may be a limitation for its use in environments where moisture exposure is frequent, as it implies a decrease in the material's long-term durability and load-bearing capacity. The behavior of CC is particularly interesting, as it exhibits a slight increase in cohesion upon saturation, rising from 3.3 MPa in the dry state to 3.6 MPa when saturated. This increase might seem counterintuitive, as water typically reduces the cohesion of concrete by acting as a lubricant. However, this increase could be due to specific characteristics of the conventional mix, where moisture may enhance the hydration of the cement, resulting in a more uniform distribution of binder materials and improving the cohesion between particles. Nevertheless, despite this slight increase, CC's cohesion remains the lowest among the three materials, indicating that it is still the least durable and resilient under both dry and saturated conditions. In a critical comparison, the results suggest that PA2 is the most robust material in terms of cohesion, demonstrating superior performance in saturated conditions. Its higher cohesion values, especially in the saturation state, make it the most suitable material for applications where high load-bearing capacity and crack resistance are essential. PA1, while slightly less cohesive in saturated, offers a good balance of performance and stability under moisture exposure, making it appropriate for environments where moisture fluctuations are moderate. CC, with the lowest cohesion values overall, may not be the best choice for environments that demand high durability and resistance to cracking, particularly in moisture-rich conditions.

The unique manufacturing process of PA2, significantly enhances its mechanical properties compared to CC. PA2's superior performance can be attributed to the higher proportion of coarse aggregate particles, direct contact between coarse aggregates, and an improved load transfer mechanism. Unlike CC, where cement paste forms a continuous matrix, PA2 relies on direct aggregate interaction, leading to better particle interlocking and stress distribution. This results in higher cohesion and an increased internal friction angle, which are critical for structural stability.

Deviator stress analysis

The analysis of deviator stress under different all-around stresses is shown in Figs. 8, 9, 10, 11 and 12. Figure 8 presents the deviator stress responses for PA1, PA2, and CC under varying all-around stress levels (5, 7.5, and 10 MPa) in the dry state. Specifically, PA2 shows superior stress resistance across all tested levels with stress values of 47.4 MPa, 67.32 MPa, and 82.04 MPa, respectively. This performance is contrasted with PA1, which exhibits lower stress tolerances at 43 MPa, 50 MPa, and 67 MPa, and CC, which manages 43.38 MPa, 54.12 MPa, and 69.61 MPa under the same stress conditions. The quantitative superiority of PA2 suggests a higher elastic limit and potentially more effective energy dissipation properties, making it particularly suitable for structural applications where high-stress resistance is required. The high performance of PA2 in a dry state indicates its potential to serve in environments where material degradation factors like moisture and temperature extremes are controlled, ensuring long-term stability and durability. This figure also serves as a compelling argument for applying TSC in high-load-bearing structures like bridges, skyscrapers, and heavy-traffic pavements where superior mechanical properties are critical.

Figure 9 contrasts the deviator stress capabilities of PA1, PA2, and CC in a saturated state. Despite the overall reduction in deviator stress due to saturation, PA2 maintaining higher stress levels at 42.07 MPa, 54.7 MPa, and 63.11 MPa across the stress levels of 5, 7.5, and 10 MPa. This is significantly better than PA1, which holds deviator stresses of 34 MPa, 40.9 MPa, and 52.1 MPa, and CC with 40.28 MPa, 48.33 MPa, and 62.79 MPa respectively.

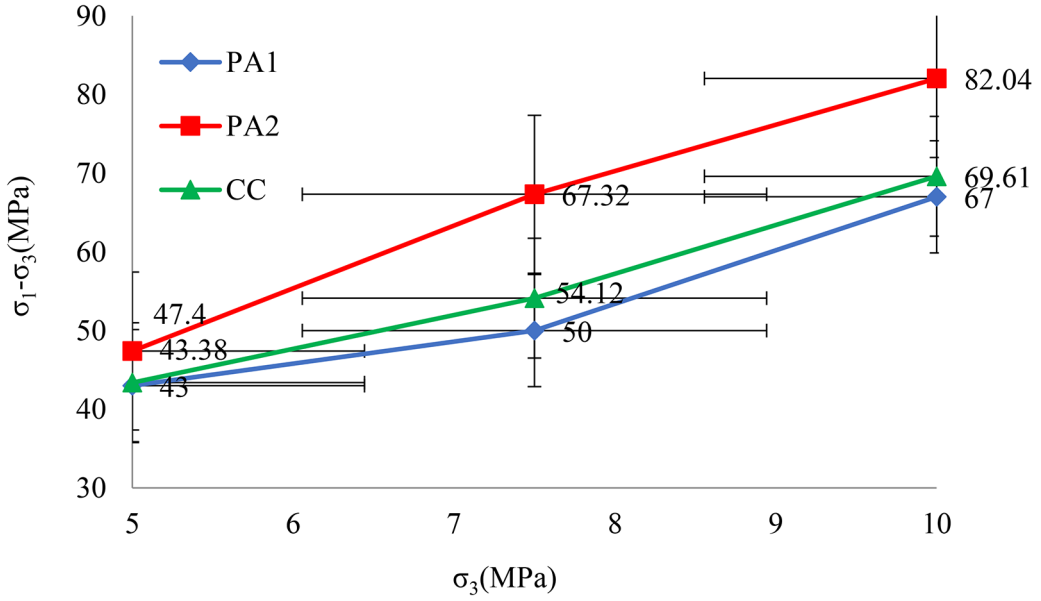

Fig. 8. Deviator stress in various all-round stresses in the dry state.

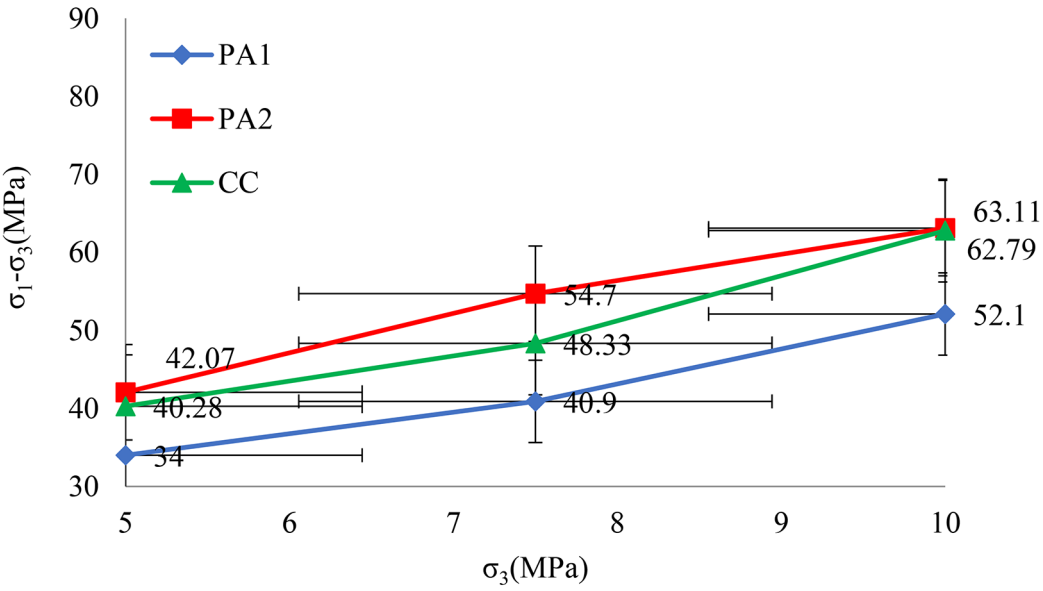

Fig. 9. Deviator stress in various all-round stresses in the saturated state.

This figure demonstrates PA2's resilience and superior performance even under challenging moisture conditions, underscoring its suitability for environments with potential for moisture exposure such as underground structures, foundations in damp soils, and regions with high humidity. The data supports the narrative that PA2's formulation, likely including moisture-resistant components or more tightly packed aggregate structures, offers enhanced durability and reliability when saturated. The relatively high performance of PA2 in saturated conditions can significantly influence construction decisions, especially in choosing materials for projects where environmental resilience is a priority.

Figure 10 focuses on the deviator stress performance of PA1 under both dry and saturated conditions. In the dry state, PA1 exhibits commendable stress tolerance under dry conditions, with deviator stress levels of 43 MPa, 50 MPa, and 67 MPa at confining pressures of 5 MPa, 7.5 MPa, and 10 MPa, respectively. However, upon saturation, these stress tolerance levels decrease to 34 MPa, 40.9 MPa, and 52.1 MPa, representing a significant reduction in the material's ability to withstand applied loads. This considerable decrease in structural capability underscores the adverse impact of moisture on PA1's mechanical properties. Under dry conditions, the internal

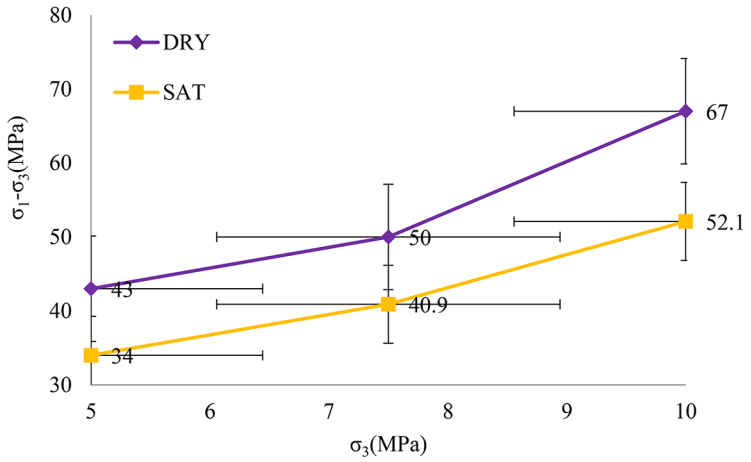

Fig. 10. Deviator stress of PA1 concrete in different all-round stresses in a dry and saturated state.

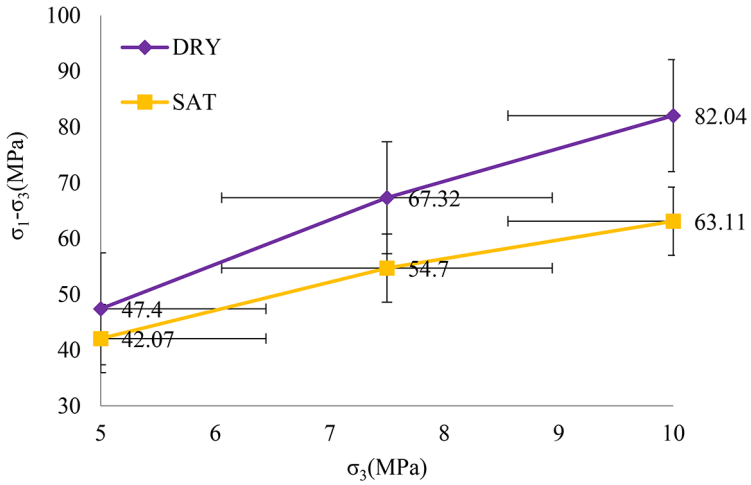

Fig. 11. Deviator stress of PA2 concrete in different all-round stresses in a dry and saturated state.

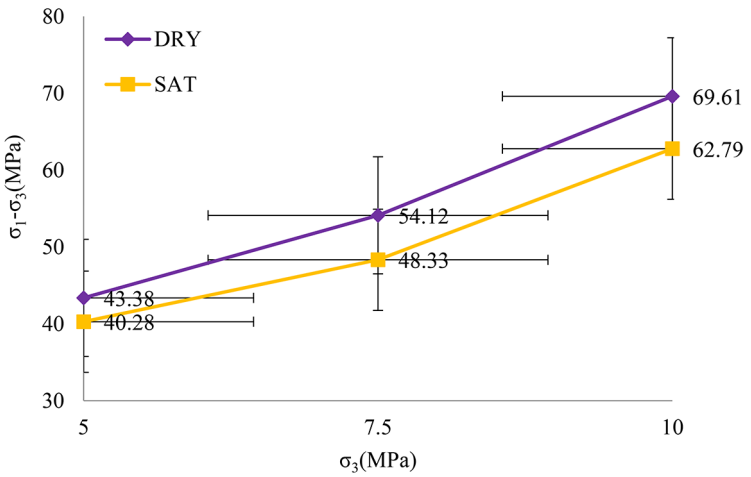

Fig. 12. Deviator stress of CC concrete in different all-round stresses in a dry and saturated state.

structure of PA1 demonstrates enhanced frictional resistance at the aggregate-cement interface, facilitating more efficient load distribution and improving its capacity to resist deviator stresses. The absence of moisture allows for the preservation of strong interfacial bonding and frictional interlock between the aggregate particles and the cement matrix, contributing to the material's elevated stress tolerance. In contrast, when PA1 is saturated, water infiltrates the micro-pores and interstitial voids, creating pore water pressure, which diminishes the material's overall load-bearing performance.

Figure 11 demonstrates PA2's exceptional ability to withstand deviator stress under both dry and saturated conditions, highlighting its superior mechanical properties and durability. Under dry conditions, PA2 achieves deviator stress values of 47.4 MPa, 67.32 MPa, and 82.04 MPa at confining pressures of 5 MPa, 7.5 MPa, and 10 MPa, respectively, showcasing its robust internal structure capable of resisting deformation and failure under applied loads. In saturated conditions, which often compromise the integrity of conventional construction materials, PA2 retains a significant portion of its strength, recording stress levels of 42.07 MPa, 54.7 MPa, and 63.11 MPa at the corresponding confining pressures. Saturation leads to reductions in stress capacity by approximately 11.25% at 5 MPa, 18.73% at 7.5 MPa, and 23.07% at 10 MPa. The deviator stress in PA2 is typically higher in dry conditions than in saturated situations due to several key factors. (i) In PAC, the composite skeleton plays a pivotal role in load distribution. In dry conditions, the direct contact between aggregate particles increases the frictional resistance, thereby enhancing the material's ability to resist deviator stresses. Conversely, in saturated environments, the formation of a water layer between the aggregates reduces friction and permits relative movement between the particles, which consequently diminishes the overall stress-bearing capacity of the material. (ii) In dry conditions, the interface between the aggregate and the cementitious matrix is strengthened by strong interfacial bonding. The absence of water in the pores promotes better adhesion and increases frictional resistance, which enables the concrete to withstand higher deviator stresses. In contrast, saturation weakens the bonding strength at the aggregate-cement interface. The infiltration of water into the micro-pores induces a lubricating effect, reducing frictional interlock and adhesion, both of which are critical for resisting applied loads. (iii) In saturated conditions, the presence of water within the pores generates pore water pressure when subjected to external stresses. This pressure opposes the confining stress, reducing the material's ability to resist deviator stresses. In contrast, in dry conditions, the absence of internal pore water pressure allows the material to fully utilize its load-bearing capacity, as there is no opposing force to hinder the distribution of applied stresses.

Figure 12 illustrates the deviator stress responses of CC under varying moisture conditions, highlighting its mechanical performance in both dry and saturated states. The results reveal that CC demonstrates a notable capacity to withstand deviator stresses in dry conditions, achieving stress values of 43.38 MPa, 54.12 MPa, and 69.61 MPa under confining pressures of 5 MPa, 7.5 MPa, and 10 MPa, respectively. However, when saturated, the stress values decrease to 40.28 MPa, 48.33 MPa, and 62.79 MPa under the same confining pressures. This reduction in deviator stress underscores the profound effect of moisture on the material's load-bearing capacity. The presence of water likely disrupts the concrete's internal microstructure by reducing the friction between aggregate particles and weakening the cement matrix's binding strength, leading to diminished resistance under external loads in saturated conditions compared to dry ones. These observations underscore the significant impact of moisture on the mechanical behavior of concrete and emphasize the importance of accounting for environmental exposure conditions in the design and application of concrete structures. Moisture-induced degradation in structural performance could adversely affect the long-term durability and safety of concrete, particularly in scenarios prone to water ingress and high confining pressures. This necessitates a comprehensive consideration of environmental factors in engineering design to ensure the reliability and service life of concrete-based constructions.

The mechanical superiority of PA2 over both PA1 and CC can be explained by its use of finer gravel and the unique two-stage process. In PA2, finer gravel increases the number of contact points between particles, enhancing the interaction between gravel, sand, and grout. This contrasts with CC, where the continuous cement matrix limits aggregate-to-aggregate interaction. The PA2 mechanism allows for superior stress transfer, reducing stress concentrations and improving resistance to deviator stress. This optimized particle interaction and stress distribution make PA2 not only stronger but also more durable under varying load conditions, solidifying its advantage over CC.

Elasticity module correlation

The module of elasticity, derived from uniaxial compressive tests, illustrates a direct relationship with compressive strength (σ), providing a predictive tool for estimating concrete elasticity based on known strength values (Fig. 13). Figure 13 is instrumental in elucidating the mechanical properties of TSC types PA1 and PA2, compared to CC. This graph presents a quantitative analysis, showing linear regression lines that depict the relationship between compressive strength (σ) and the modulus of elasticity (E) for each concrete type, effectively demonstrating how material stiffness increases with strength. The regression lines are defined as follows:

$$PA1 : E = 0.9471\sigma + 3.3588 \; with \; R^2 = 0.793 \tag{5}$$

$$PA2 : E = 1.0895\sigma + 0.7028 \; with \; R^2 = 0.939 \tag{6}$$

$$CC : E = 0.409\sigma + 10.354 \; with \; R^2 = 0.9661 \tag{7}$$

The slope of the regression line for PA2 is notably steeper than that for PA1 and CC. This implies that PA2 has a higher modulus of elasticity at any given compressive strength and gains more stiffness per unit of strength increase than PA1 or CC. This characteristic makes PA2 exceptionally suited for structural applications where deflections are critical, such as in tall structures where vertical stiffness is paramount to prevent sway and

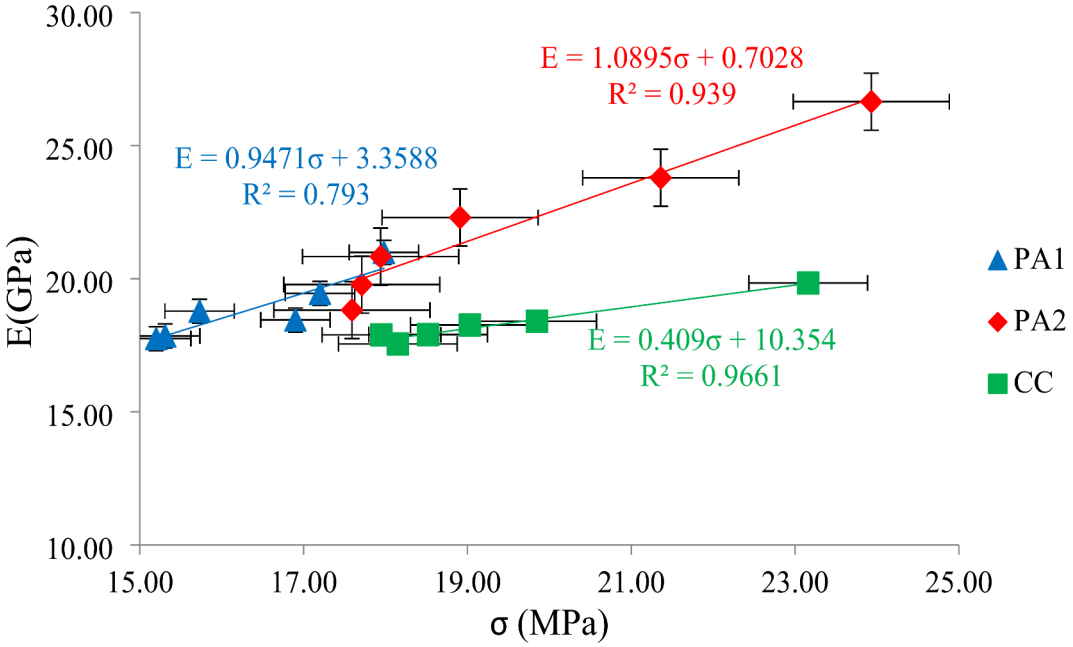

Fig. 13. The relations between compressive strength (σ) and module of elasticity (E) for TSC and CC.

ensure stability. The high R^2 values, especially for PA2 and CC, indicate a strong linear relationship between compressive strength and modulus of elasticity. This strong correlation means that once the compressive strength of the concrete is known, its stiffness can be predicted with high accuracy, which is invaluable in the design phase of construction projects. The relationships depicted in Fig. 13 allow for the optimization of concrete mixes. By tweaking components such as aggregate size, the type of cement, and admixtures, manufacturers can refine their concrete to enhance strength and stiffness. This is particularly relevant for PA2, suggesting that its mix design could be further optimized to push the boundaries of strength and stiffness. Overall, the detailed exploration of the relationships in Fig. 13 underscores the complex interplay between material properties that are pivotal to the engineering and construction industries. It highlights how advanced materials like PA2 set new benchmarks in the field, offering enhanced capabilities that can significantly impact the design and execution of future construction projects.

The findings of this research offer significant potential for advancing the simulation of TSC, as the essential parameters for concrete modeling and simulation were experimentally determined in a laboratory setting. These results contribute to cost reduction and enhance the efficiency of analyzing the mechanical properties of TSC, ultimately enabling faster and more economical simulation processes.

Conclusion

This comprehensive research provides an in-depth comparative analysis of the triaxial compressive strength and associated mechanical properties between TSC and CC. Here, we summarize the critical findings and explore their broader implications through quantitative analysis:

- The aggregate size significantly impacts concrete's shear strength. Notably, TSC (PA2) with finer aggregates achieved higher shear strengths, reaching 52.4 MPa at 5 MPa confining pressure in dry conditions, compared to 43 MPa for PA1 and 43.38 MPa for CC. This indicates that finer aggregates are crucial for optimizing concrete's mechanical properties, improving shear resistance, and enhancing the overall durability and load-bearing capacity of structures.
- The comparative analysis between TSC and CC under varied moisture conditions revealed a differential response, with all materials exhibiting reduced strength when saturated. For example, under a confining pressure of 5 MPa, PA2 maintained a higher deviator stress tolerance in a saturated state at 42.07 MPa, compared to 40.28 MPa for CC and 34 MPa for PA1.
- TSC showed exceptional stress tolerance due to its composition and aggregate granularity. Specifically, PA2 demonstrated superior deviator stress tolerance, reaching up to 82.04 MPa under dry conditions at a 10 MPa confining pressure, significantly surpassing PA1 (67 MPa) and CC (69.61 MPa).
- TSC's higher internal friction angles indicate improved shear resistance compared to CC. For example, PA2 exhibited an internal friction angle of 51degree in dry conditions, outperforming PA1 (44.9 degree) and CC (46.4 degree). This characteristic highlights TSC's potential for applications requiring high shear strength, contributing to safer and more durable structures.
- TSC displays a higher modulus of elasticity compared to CC, indicating better deformation behavior under stress. The relationship between compressive strength and modulus of elasticity for PA2 shows a steep slope with a high R^2 value of 0.939, suggesting that elasticity can be reliably predicted from known strength values.

This property enhances TSC's suitability for a wider range of structural applications, ensuring improved reliability and structural integrity in load-bearing components.

In conclusion, the study substantiates TSC's superior properties and calls for a paradigm shift in how construction materials are chosen and utilized, especially in critical infrastructure projects. Further research should focus on optimizing TSC formulations for specific applications, exploring cost-effective production methods, and evaluating long-term performance to fully harness the benefits of this innovative material in the construction industry.

Data availability

Data availabilityThe datasets used and/or analysed during the current study available from the corresponding author on reasonablerequest.

Received: 2 June 2024; Accepted: 25 November 2024
Published online: 26 November 2024

References

1. Mohan, K. S. R., Diviyabharrathi, K. B. & Murali, G. Research on the development of high impact resistant Preplaced Aggregate fibrous concrete by the Inclusion of Coarse Aggregates Coated with asphalt. *Arab. J. Sci. Eng.* **47**, 4265–4286 (2022).
2. Rajabi, A. M., Moaf, O., Abdelgader, H. S. & F. & Evaluation of Mechanical properties of two-stage concrete and conventional concrete using nondestructive tests. *J. Mater. Civ. Eng.* **32**, 04020185 (2020).
3. Prasad, N. & Murali, G. Research on flexure and impact performance of functionally-graded two-stage fibrous concrete beams of different sizes. *Constr. Build. Mater.* **288**, 123138 (2021).
4. Najjar, M. F., Soliman, A. M. & Nehdi, M. L. Critical overview of two-stage concrete: Properties and applications. *Constr. Build. Mater.* **62**, 47–58 (2014).
5. Ramakrishnan, K. et al. Standard and modified falling mass impact tests on preplaced aggregate fibrous concrete and slurry infiltrated fibrous concrete. *Constr. Build. Mater.* **298**, (2021).
6. Tuyan, M., Zhang, L. V. & Nehdi, M. L. Development of sustainable alkali-activated slag grout for preplaced aggregate concrete. *J. Clean. Prod.* **277**, (2020).
7. 304.1-R. A. C. I. Guide for the Use of Preplaced aggregate concrete for structural and Mass concrete applications. *ACI Mater. J.* **88**, (1992).
8. Balmer, G. G. Shearing strength of concrete under high triaxial stress-computation of Mohr's envelope as a curve. *Report No. SP-23, Structural Research Laboratory Report, Bureau of Reclamation, United States Department of the Interior* (1949).
9. Vieira, M., Bettencourt, A., Camelo, A. & Ferreira, J. Self-compacting mortar for mass concrete application with PAC technology. *Scc2010* (2010).
10. Abdelgader, H. S. & Górski, J. Influence of grout proportions on modulus of elasticity of two-stage concrete. *Magazine Concrete Res.* **54**, 251–255 (2002).
11. Abdelgader, H. S. Effect of the quantity of sand on the compressive strength of two-stage concrete. *Magazine Concrete Res.* **48**, 353–360 (1996).
12. Ichino, H., Kuwahara, N., Beppu, M., Williamson, E. B. & Himi, A. Effects of the shape, size, and surface roughness of glass coarse aggregate on the mechanical properties of two-stage concrete. *Constr. Build. Mater.* **411**, (2024).
13. Das, K. K., Lam, E. S. S., Ip, C. T., Chau, Y. K. & Jang, J. G. Modified pull-off test evaluation of bond properties in preplaced aggregate concrete incorporating silica fume. *J. Building Eng.* **82**, (2024).
14. Das, K. K., Lam, E. S. S. & Jang, J. G. Effects of modified binders on flowability of grout and properties of preplaced aggregate concrete. *J. Building Eng.* **68**, (2023).
15. Esmaeili, M. & Amiri, H. Laboratory Investigation into the Flexural Behavior of embedded concrete sleepers in two-stage concrete with Preplaced Ballast Aggregate. *Int. J. Concrete Struct. Mater.* **16**, (2022).
16. Li, P. P., Yu, Q. L., Brouwers, H. J. H. & Chen, W. Conceptual design and performance evaluation of two-stage ultra-low binder ultra-high performance concrete. *Cem. Concr. Res.* **125**, (2019).
17. Bayer, R. İ. Use of preplaced aggregate concrete for mass concrete applications. (2004).
18. Murali, G. et al. Combined effect of multi-walled carbon nanotubes, steel fibre and glass fibre mesh on novel two-stage expanded clay aggregate concrete against impact loading. *Crystals* **11**, (2021).
19. Vatin, N. I. et al. Enhancing the impact strength of prepacked aggregate fibrous concrete using asphalt-coated aggregates. *Materials* **15**, (2022).
20. Murali, G., Parthiban, K., Wong, L. S., Abid, S. R. & Nassar, A. K. Enhanced impact properties of functionally graded preplaced aggregate fibrous concrete slabs comprising alkali-activated slag and carbon nanotube grout. *J. Building Eng.* **82**, (2024).
21. Ichino, H., Beppu, M. & Williamson, E. B. Blast-resistant performance of a two-stage concrete plate subjected to contact explosions. *Constr. Build. Mater.* **259**, (2020).
22. Wang, H. & Song, Y. Behavior of dam concrete under biaxial compression-tension and triaxial compression-compression-tension stresses. *Front. Archit. Civil Eng. China*. **2**, 323–328 (2008).
23. Vu, X. D., Briffaut, M., Malecot, Y., Daudeville, L. & Ciree, B. Influence of the saturation ratio on concrete behavior under triaxial compressive loading. *Science and Technology of Nuclear Installations* (2015). (2015).
24. Chen, Q., Zhang, Y., Zhao, T., Wang, Z. & Wang, Z. Mesoscale modelling of concretes subjected to triaxial loadings: mechanical properties and fracture behaviour. *Materials* **14**, 1–25 (2021).
25. Su, B., Zhou, Z., Li, Z., Wang, Z. & Shu, X. Experimental investigation on the mechanical behavior of foamed concrete under uniaxial and triaxial loading. *Constr. Build. Mater.* **209**, 41–51 (2019).
26. Liu, M. et al. Strength and deformation performances of silt-based foamed concrete under triaxial shear loading. *J. Building Eng.* **60**, (2022).
27. Ashrafi, E. & Farzam, M. Experimental investigation on the triaxial behavior of lightweight concrete. *Constr. Build. Mater.* **312**, (2021).
28. ASTM C192/C. 192 M – 19, Standard Practice for Making and Curing Concrete Test Specimens in the Laboratory.
29. ASTM-C470-C470M-23. Standard Specification for Molds for Forming Concrete Test Cylinders Vertically.
30. C 801–98. Standard Test Method for Determining the Mechanical Properties of Hardened Concrete Under Triaxial Loads.
31. Hsieh, P. A. Jaeger, L., & Cook, N. G. W. *(* Fundamentals of rock mechanics (3rd ed.). Chapman and Hall. Geofluids vol. 9 (2009). (1979).
32. Al-Awad, M. N. J. Simple correlation to Evaluate Mohr-Coulomb failure Criterion using Uniaxial Compressive Strength. *J. King Saud Univ. - Eng. Sci.* **14**, 137–144 (2002).

33. Coulomb, C. A. Essai sur une application des regles de maximis et minimis a quelques problemes de statique relatifs a l'architecture Mémoires Math Phys Acad. *Roy Sci.* **1776**, 343–382 (1973).

Acknowledgements
The authors of the article express their appreciation and thanks to, Eng. Bahman Pirhadi and Eng. Fatemeh Omidi Moaf who have cooperated in various stages of this research.

Author contributions
Hakim S. Abdelgader led the conceptualization of the research framework and designed the experimental protocols. As the principal investigator, Hakim was pivotal in overseeing the project's execution. He also played a significant role in the supervision of the research team.Ali M. Rajabi and Farzam Omidi Moaf were primarily responsible for the data collection and the initial analysis phase. Their expertise was crucial in conducting the triaxial compressive strength tests and ensuring the accuracy and reliability of the data gathered.Marzena Kurpińska took the lead in data analysis, applying advanced statistical methods to interpret the results. Her contributions were vital in translating raw data into actionable insights that shaped the study's outcomes.Gunasekaran Murali was tasked with drafting the initial manuscript. He integrated inputs from all co-authors and ensured that the manuscript reflected the study's findings accurately and comprehensively.Mikołaj Miśkiewicz and Farzam Omid Moaf were responsible for creating all the visual representations of data, including figures and tables. Their work was essential in clearly presenting complex data and enhancing the manuscript's overall impact.All authors reviewed the manuscript, provided critical feedback, and approved the final version for publication. They also engaged in regular discussions that guided the study's progress and addressed any challenges that arose during the research process.

Declarations

Competing interests
The authors declare no competing interests.

Additional information
Supplementary Information The online version contains supplementary material available at https://doi.org/10.1038/s41598-024-81112-8.

Correspondence and requests for materials should be addressed to H.S.A.

Reprints and permissions information is available at www.nature.com/reprints.

Publisher's note Springer Nature remains neutral with regard to jurisdictional claims in published maps and institutional affiliations.